Effects of RF Pulses on Circuits and Systems
---- Pieces-----

J. L. Volakis, E. Siah, T. Yang and V. Liepa
Radiation Laboratory
Dept. of Electrical Engineering and Computer Science
University of Michigan
Ann Arbor, MI. 48109-2122

Phone: (734)647-1797, Fax: (734)647-2106
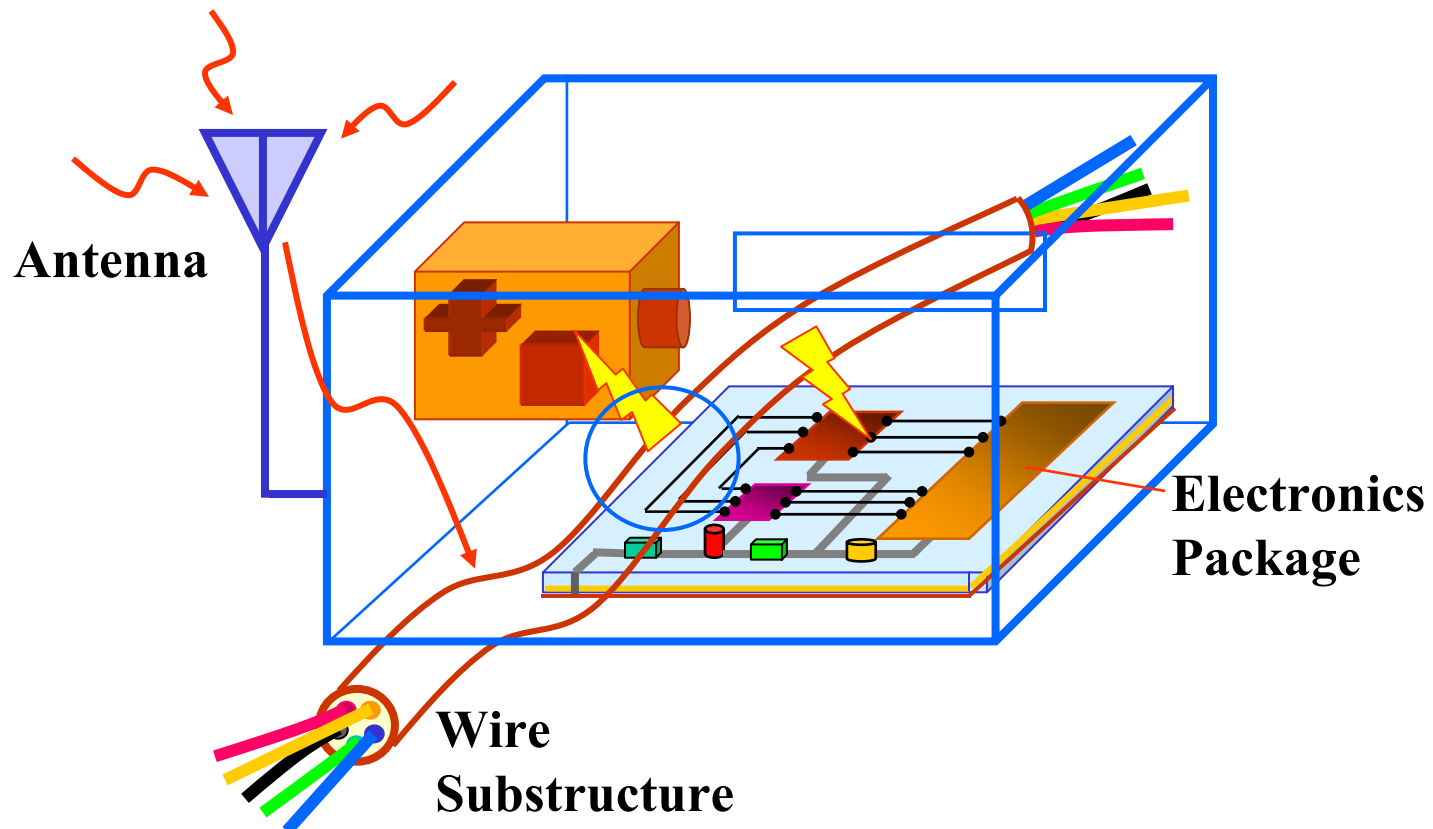Email: volakis@umich.edu
http://www-personal.engin.umich.edu/~volakis/
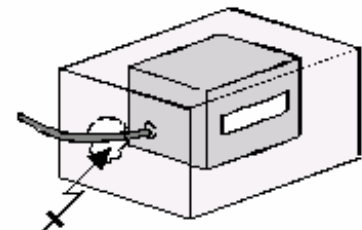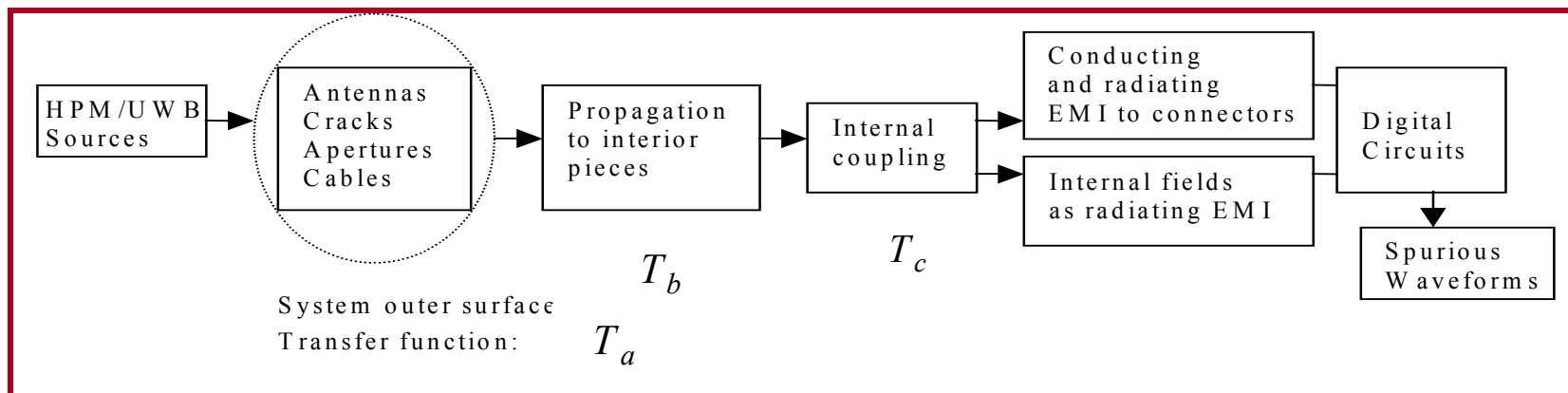
Annual RF Effects MURI Review

Report Documentation Page

1. REPORT DATE **JUN 2002**	2. REPORT TYPE **N/A**	3. DATES COVERED **-**		
4. TITLE AND SUBTITLE **Effects of RF Pulses on Circuits and Systems -Pieces-**		5a. CONTRACT NUMBER		
		5b. GRANT NUMBER		
		5c. PROGRAM ELEMENT NUMBER		
6. AUTHOR(S)		5d. PROJECT NUMBER		
		5e. TASK NUMBER		
		5f. WORK UNIT NUMBER		
7. PERFORMING ORGANIZATION NAME(S) AND ADDRESS(ES) **Radiation Laboratory Dept. of Electrical Engineering and Computer Science University of Michigan Ann Arbor, MI. 48109-2122**		8. PERFORMING ORGANIZATION REPORT NUMBER		
9. SPONSORING/MONITORING AGENCY NAME(S) AND ADDRESS(ES)		10. SPONSOR/MONITOR'S ACRONYM(S)		
		11. SPONSOR/MONITOR'S REPORT NUMBER(S)		
12. DISTRIBUTION/AVAILABILITY STATEMENT **Approved for public release, distribution unlimited**				
13. SUPPLEMENTARY NOTES **Presentations given at the First Annual Review Meeting on June 8, 2002 DoD MURI Award F49620-01-1-0436, The original document contains color images.**				
14. ABSTRACT				
15. SUBJECT TERMS				

16. SECURITY CLASSIFICATION OF:			17. LIMITATION OF ABSTRACT	18. NUMBER OF PAGES	19a. NAME OF RESPONSIBLE PERSON
a. REPORT **unclassified**	b. ABSTRACT **unclassified**	c. THIS PAGE **unclassified**	**UU**	**32**	

Project Statement

- Evaluate the response/induced voltages on electrical systems due to radiated EM field environments
  - Focus is on upset or damage of digital systems
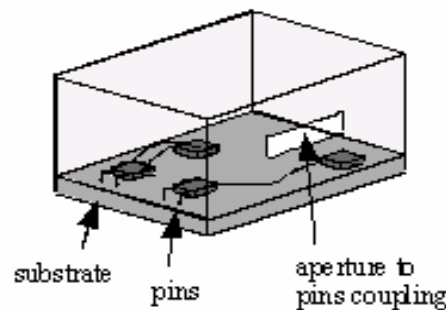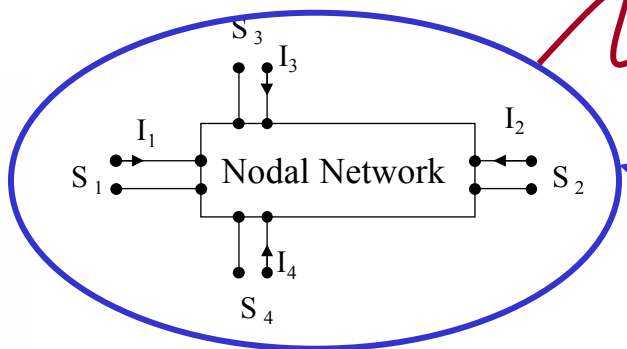 - For fast transient or pulsed CW excitations at GHz frequencies

Antenna

Electronics Package

Wire Substructure

HPM/UWB Sources

Antennas
Cracks
Apertures
Cables

Propagation to interior pieces

Internal coupling

Conducting and radiating EMI to connectors

Internal fields as radiating EMI

Digital Circuits

Spurious Waveforms

T_b

T_c

System outer surface
Transfer function: T_a

S_3
I_3
I_1
S_1
Nodal Network
I_2
S_2
I_4
S_4

box to box / aperture to aperture coupling

(e) Nested Boxes

substrate pins aperture to pins coupling

(f) aperture to circuit pins

Numerically model penetration and coupling of HPM and UWB sources into large-scale, complex structures

- Employ frequency domain and time domain methods.
- Decompose structure into pieces
  - Black boxes with pins/connectors
  - Cable bundles;
  - Cavities with apertures
  - Cavities containing cable bundles
  - Antennas as direct (front door) and out-of-band (back door) entry ports
  - Aperture with cable bundle passing through;
  - Aperture in cavity with cable bundle passing through;
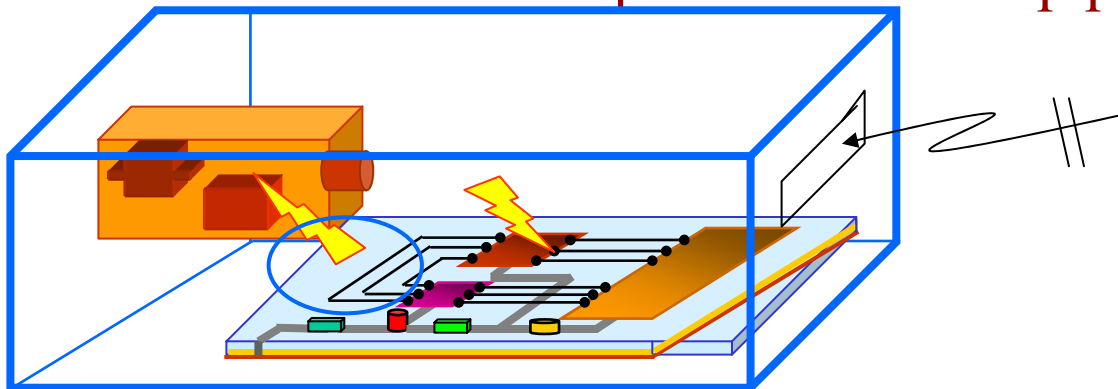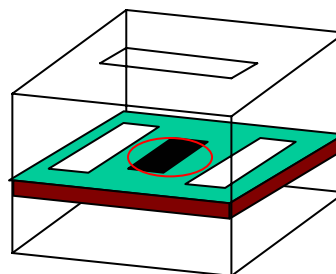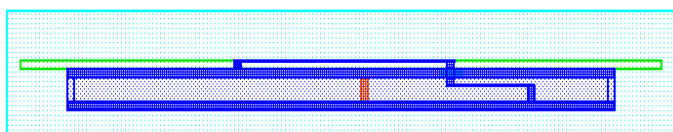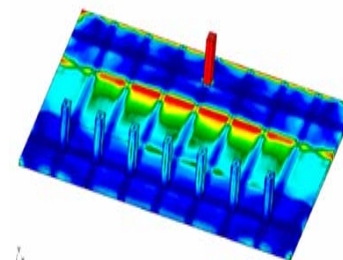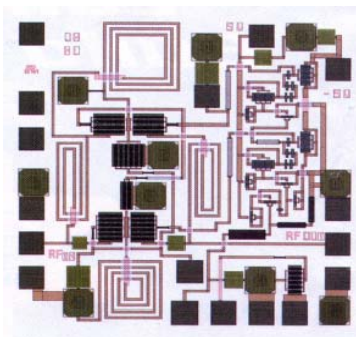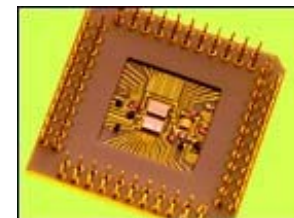 - Seams in surfaces;

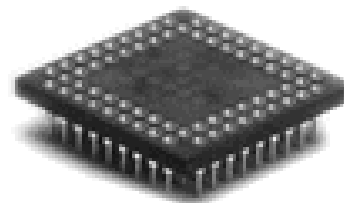- Characterization of RF coupling into cavity structures using multilevel FMM (SIE) with
  - Apertures
  - With cables

- Phenomenology and shielding studies

- Simplified Circuit characterizations for integration into Topology/BLT model

- Initiated development of hybrid finite element-boundary method for general purpose analysis of enclosed RF circuits

Goal is to evaluate field responses at the chip pins
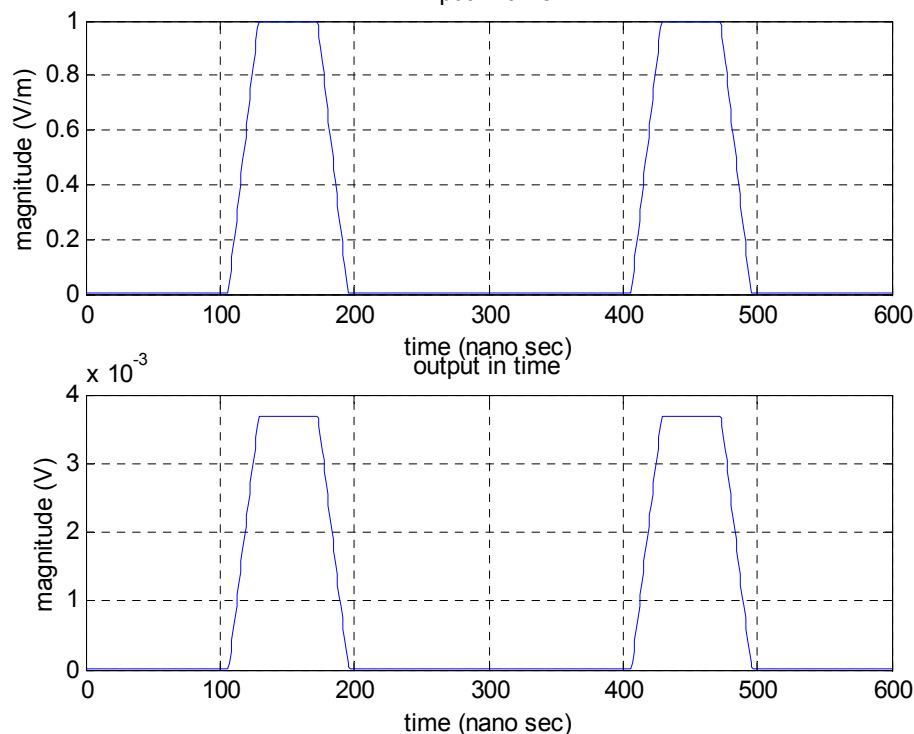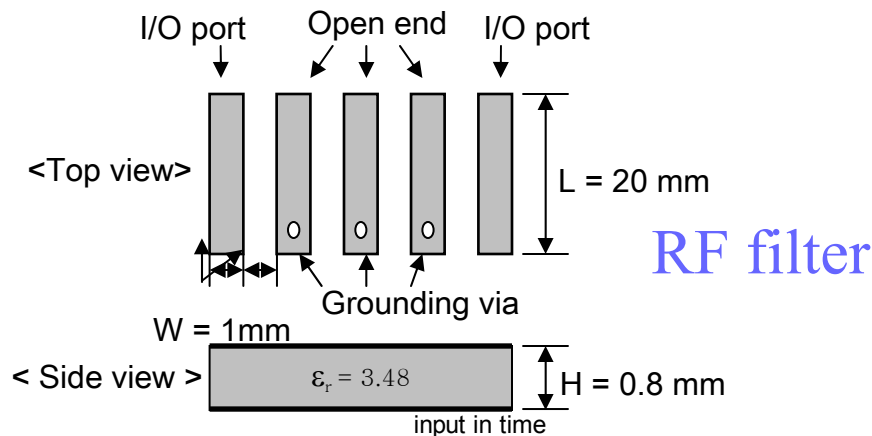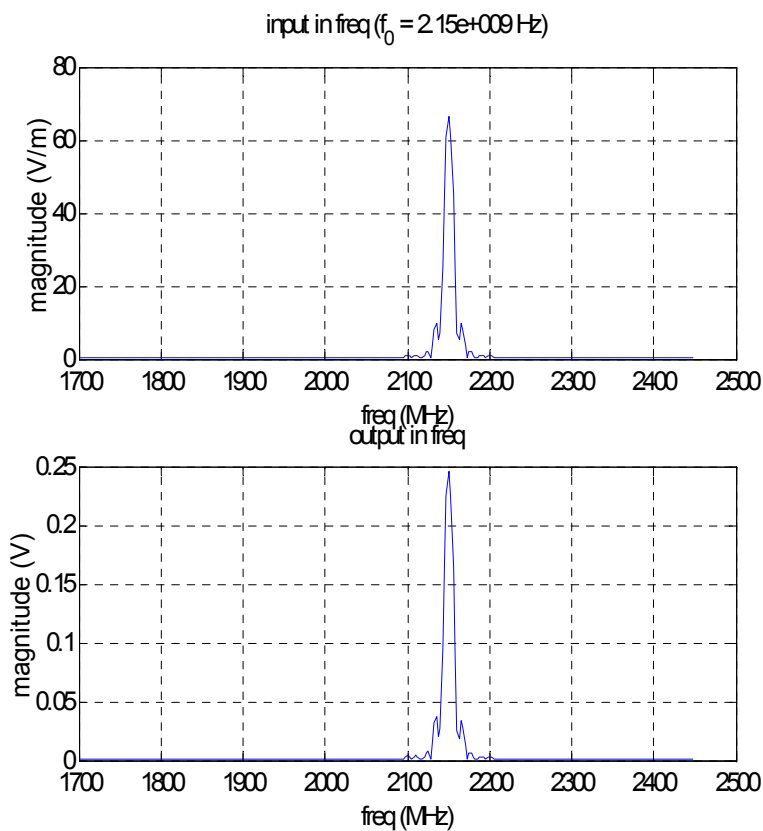
- High speed devices generate coupling and interference
  - Radiation from chip surfaces
  - Conduction noise from signal ports
  - Power-line conducting noise
- EMI from surrounding electronic environment.
- Cavity enclosures may cause reverberations that enhance interference, particularly at exposed wiring
- Intentional sources can cause significant high fields to disrupt logic functions

Input in time domain : 100 V/m
Output in time domain : 0.4 V
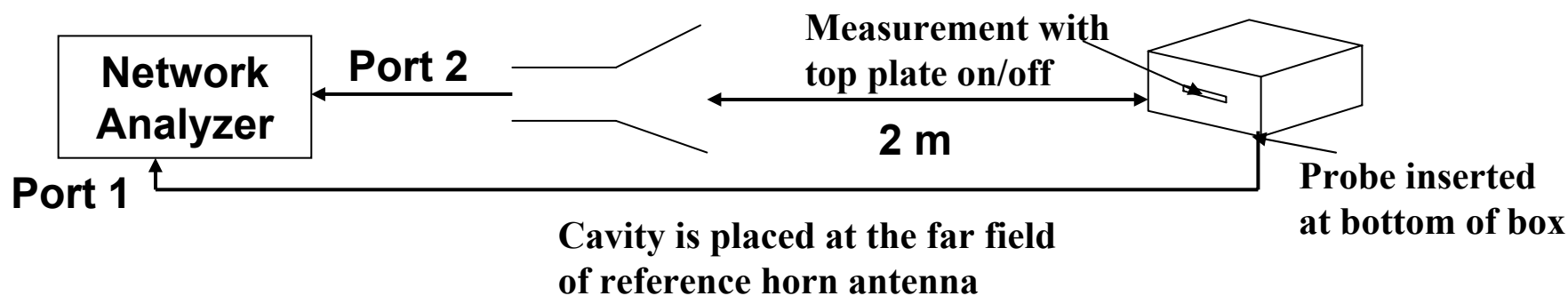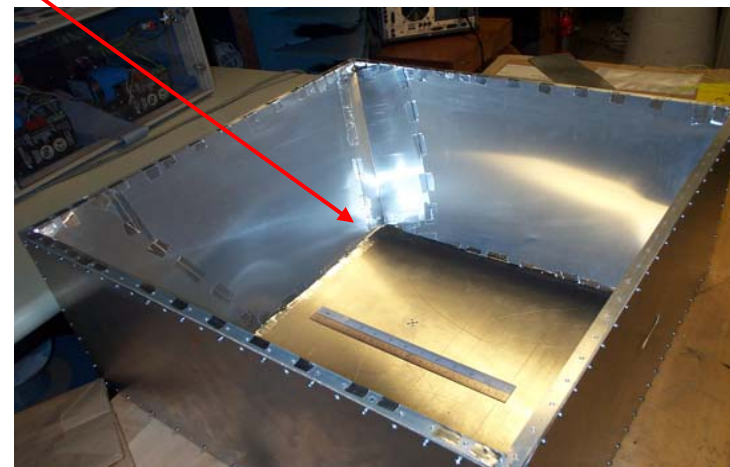

input in freq ($f_0 = 2.15e+009$ Hz)

output in freq

I/O port   Open end   I/O port

<Top view>

L = 20 mm

RF filter

Grounding via

W = 1mm

< Side view > $\varepsilon_r = 3.48$ H = 0.8 mm

input in time

output in time

Cavities Can Cause Amplification

Impinging plane wave from the ambient environment

Circuit Substrate

Circuit elements eg. Filters, mixers oscillators.

V_{SS}

V_+

Analog Integrated Circuit with pins connected to circuit traces

V_{DD}

V_-

Circuit elements eg. Filters, mixers oscillators.

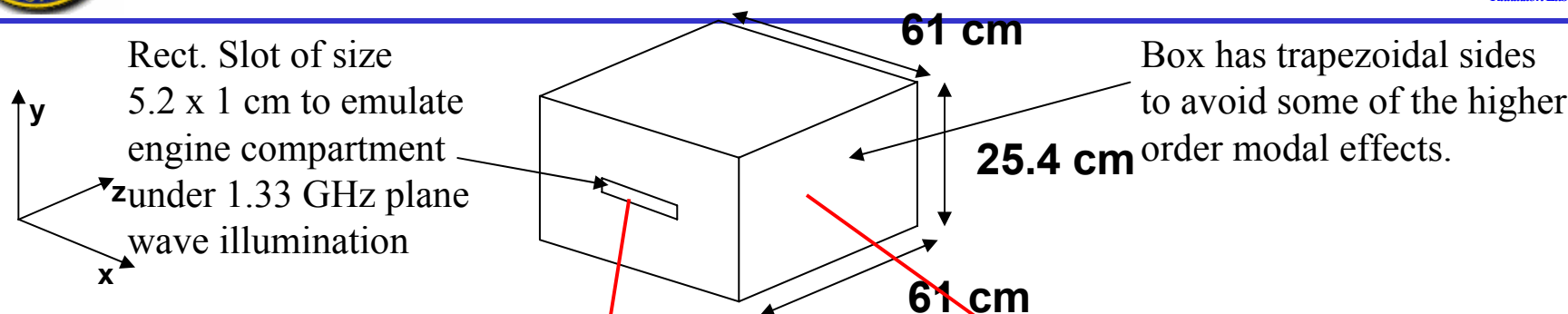V_{output}

Ground

➤ Cavities can exhibit a resonance amplification of 10 to 20 dB amplification of the ambient radiation.

➤ Amplification of signals can have a significant impact on circuits with Analog ICs and high frequency amplifiers.

➤ Induced voltage fluctuations on ground, power supply and signal lines can change circuit devices performance.

Measured Over-Moded Cavity

Rect. Slot of size 5.2 x 1 cm to emulate engine compartment under 1.33 GHz plane wave illumination

Box has trapezoidal sides to avoid some of the higher order modal effects.

61 cm

25.4 cm

61 cm

Network Analyzer

Port 2

Port 1

Measurement with top plate on/off

2 m

Probe inserted at bottom of box

Cavity is placed at the far field of reference horn antenna
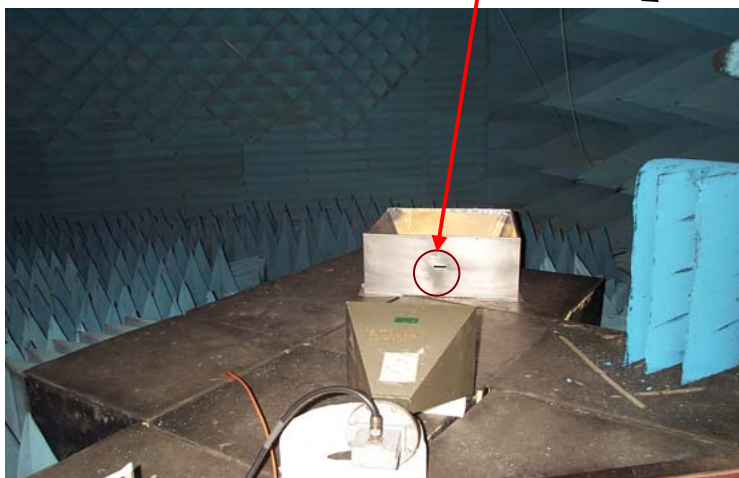
• Measured data is Transmission S12 with the Horn Antenna connected to Port 2 and the field Probe connected to Port 1 in dB.

• Measured with the top cover on and without the top cover.

• Absence of top cover avoids most of the higher order resonances.

Cover on

Cover off

15 dB higher with cavity fully closed
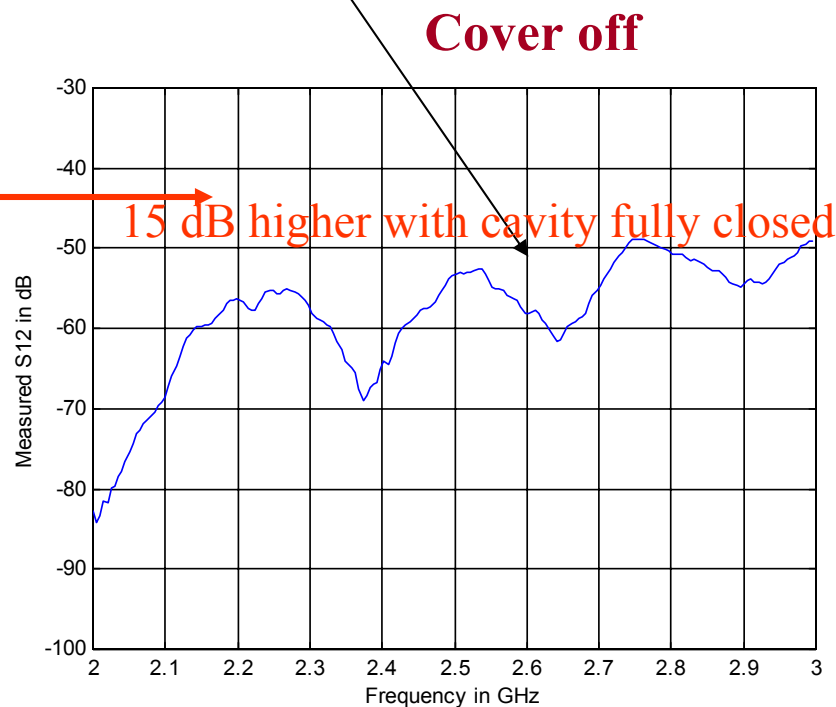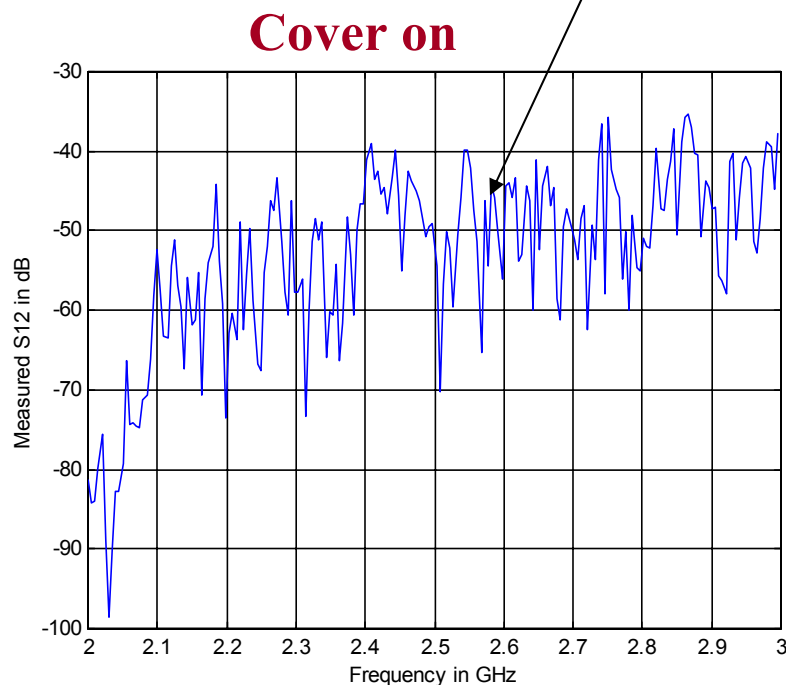
• **Electric Field Shielding**

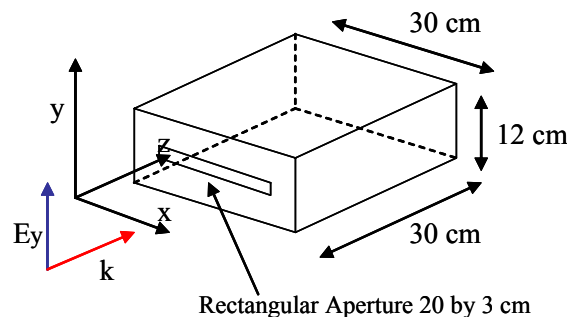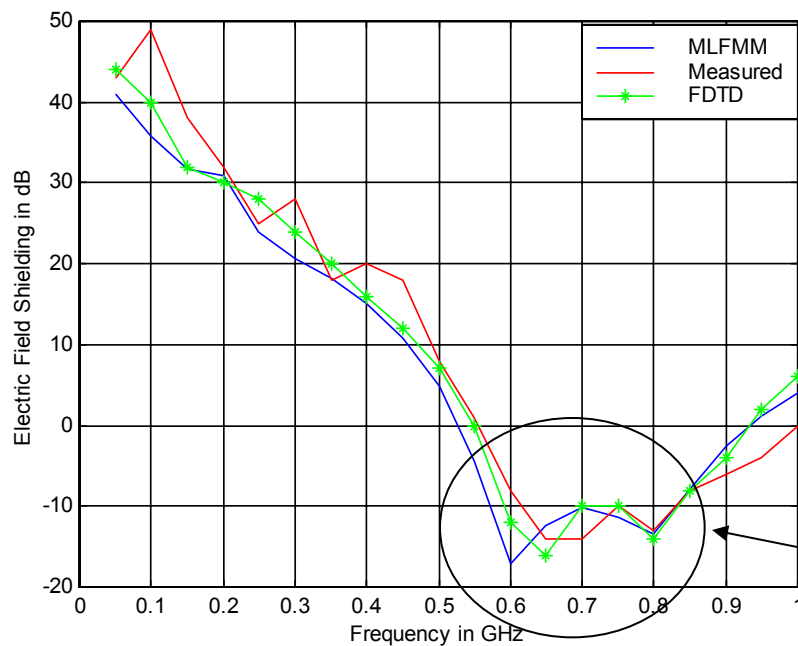$$\text{EFS} = -20\log\left|\frac{E^{\text{total}}}{E^{\text{inc}}}\right| \quad (\text{dB})$$

• **Magnetic Field Shielding**

$$\text{MFS} = -20\log\left|\frac{H^{\text{total}}}{H^{\text{inc}}}\right| \quad (\text{dB})$$

where E/H^{total} is the total E/H field in the presence of the scattering object and E/H^{inc} is the incident E/H field in the absence of the scattering object.

• EFS and MFS are parameters to indicate the degree of coupling from external illumination to points within a cavity. Higher values indicate better shielding and thus weaker total field values.

• Ratio of the Stored Electric/Magnetic Energy within the volume of the cavity of the total fields to the incident fields.

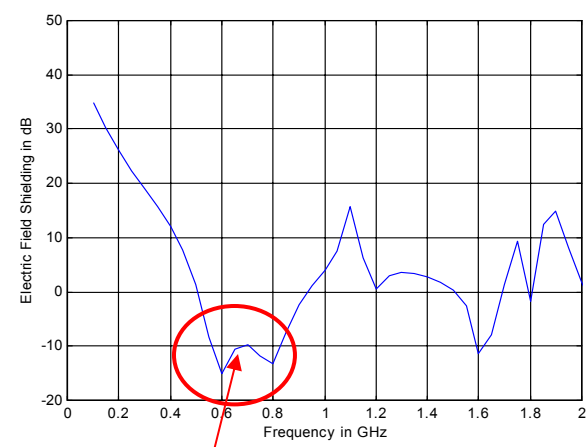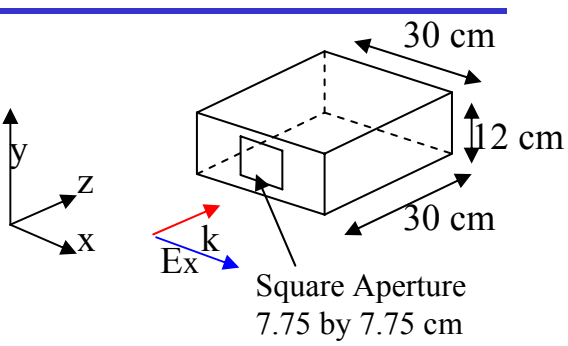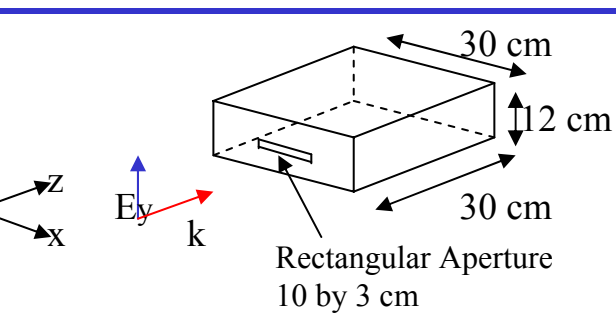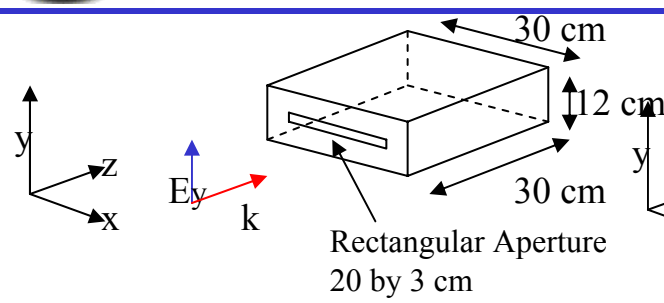• EFS and MFS are computed using the multi-level FMM code EMCAR.

- Rectangular slot in a 30cmx30cmx12cm cavity (slot size 20x3cm)

Rectangular Aperture 20 by 3 cm

Slot resonance (0.75 GHz)

The first resonance (0.7GHz) of the lowest order mode in the cavity

30 cm

12 cm

30 cm

Rectangular Aperture
20 by 3 cm

E_y

30 cm

12 cm

30 cm

Rectangular Aperture
10 by 3 cm

E_y

30 cm

12 cm

30 cm

Square Aperture
7.75 by 7.75 cm

E_x

**Slot + TE$_{101}$
resonance**

TE$_{101}$ resonance

TE$_{011}$ resonance

Slot resonance

Slot resonance

E_y Polarization

E_y Polarization

E_x Polarization

Electric Field Shielding for the 2 wire configurations
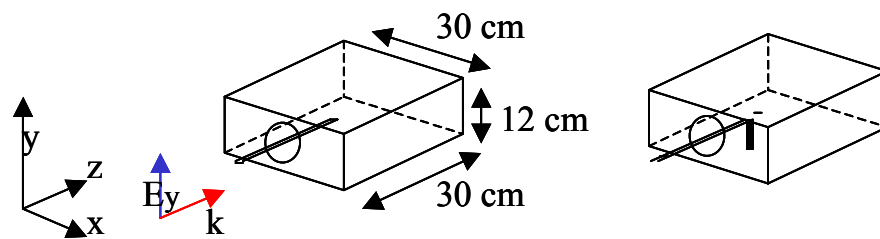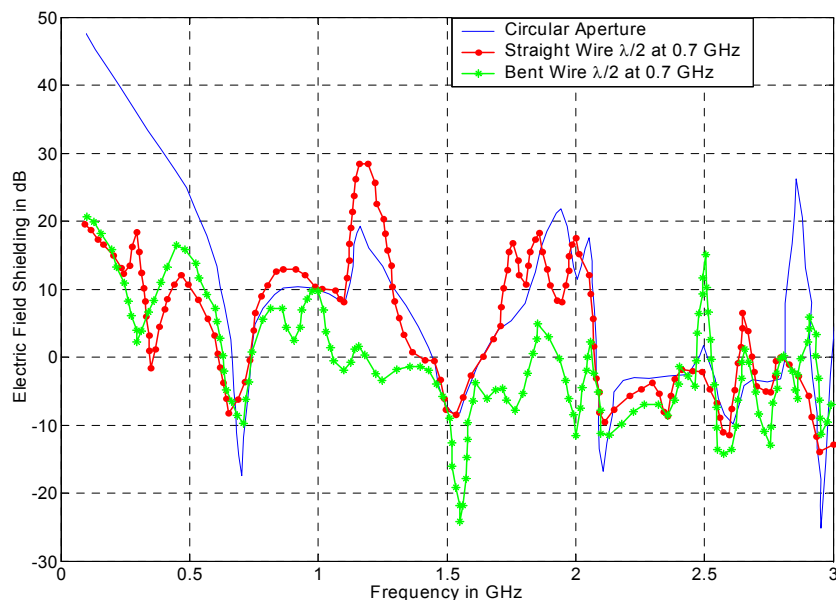
> Presence of wires changes significantly the shielding characteristic of a resonant metallic cavity.
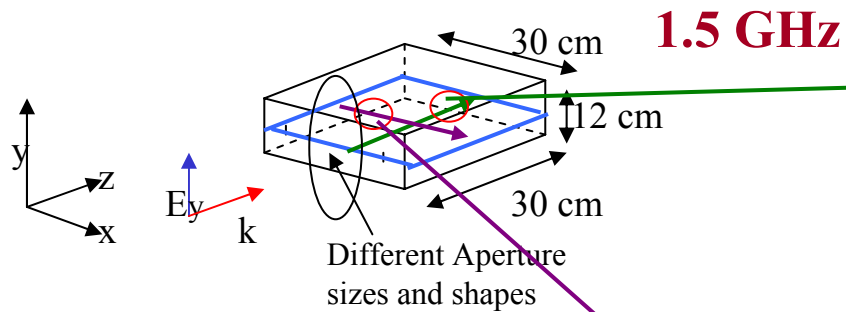
> Bent and longer wire configurations couple more energy from external illumination into the metallic enclosure.

> Increase in coupled energy due to wire penetrations poses a challenge to proper circuit device performance.

1.5 GHz

30 cm

12 cm

30 cm

Different Aperture sizes and shapes

Ey k

y z x

Combination of slot and cavity resonance at 1.5 GHz

EFS distribution for square slot at 1.5 GHz

1.5 GHz
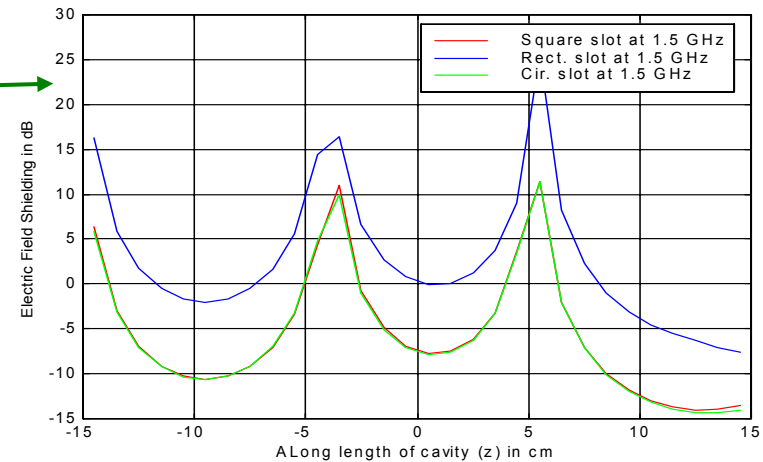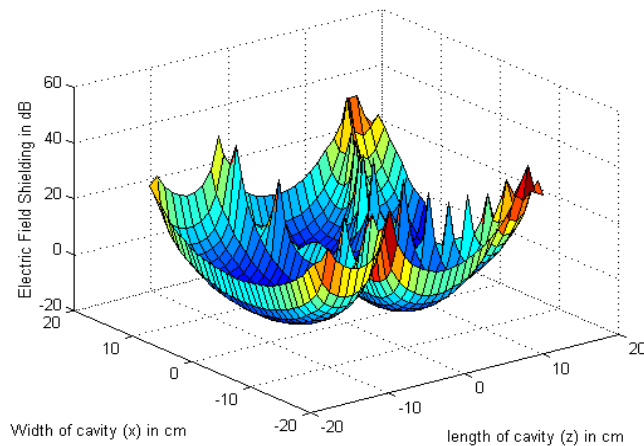
Back of cavity   **Radiating Aperture**

What is Important?
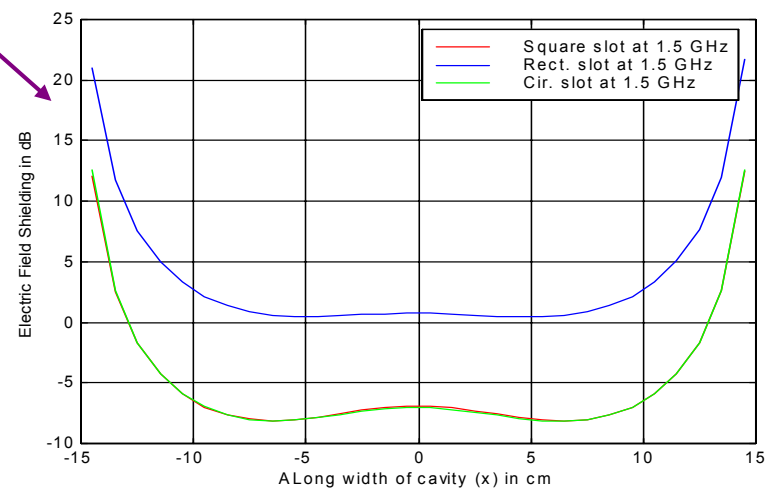
- **Cavity resonances**
- **Slot resonances**
- **Resonances of other substructures (wires, other arbitrary apertures, protrusions)**
- **Interactions between Cavity, Slot and Wire resonances**

Rectangular slot
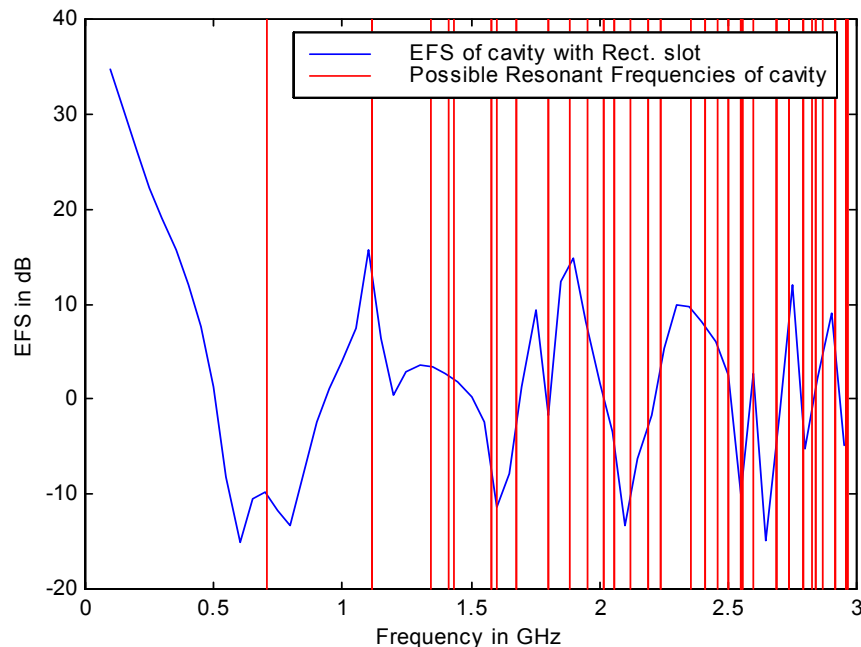
Circular slot
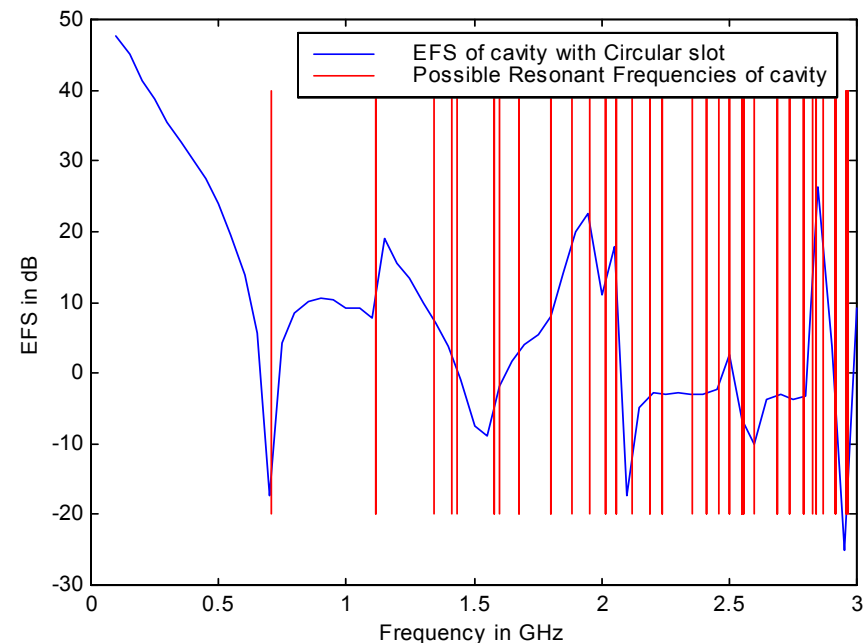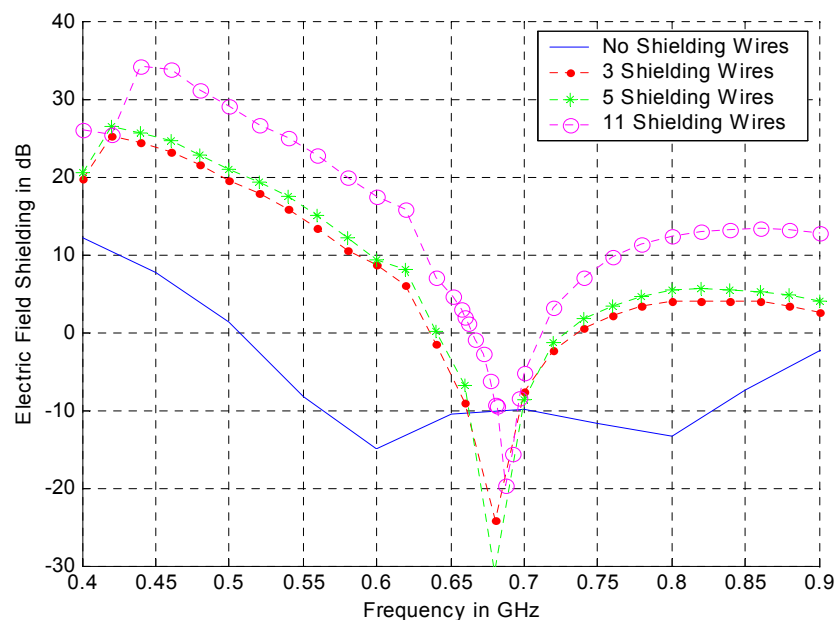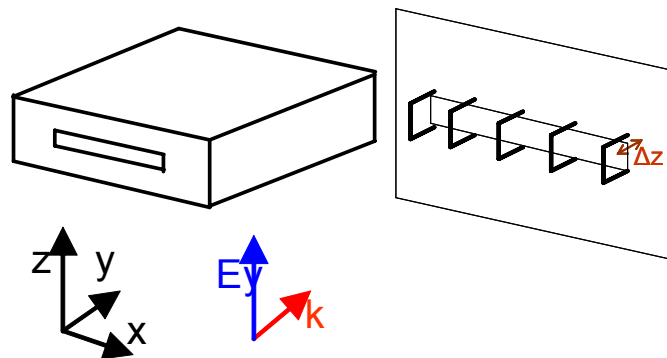
Variation in Number of Wires with ΔZ = 3cm
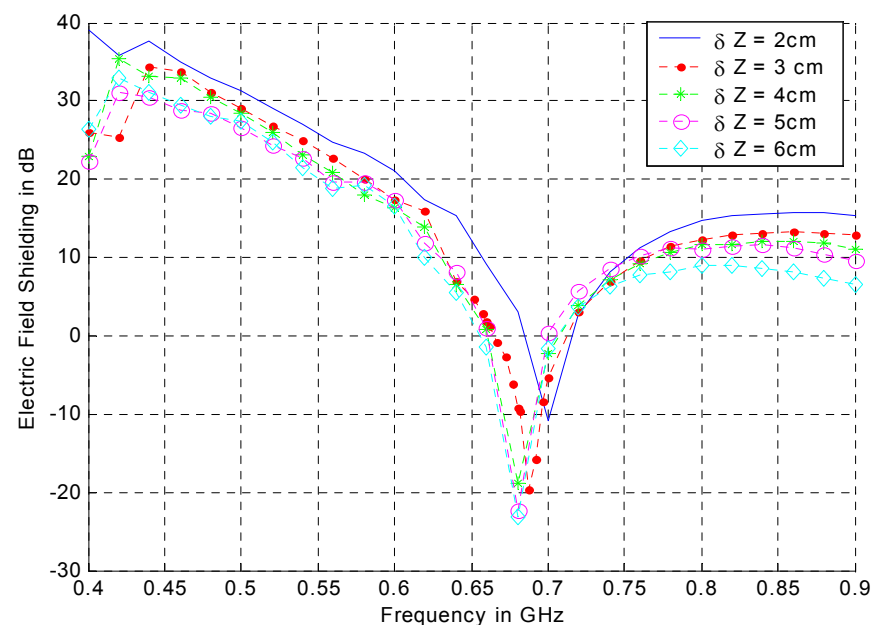
Variation in Distance ΔZ of Wire from Slot
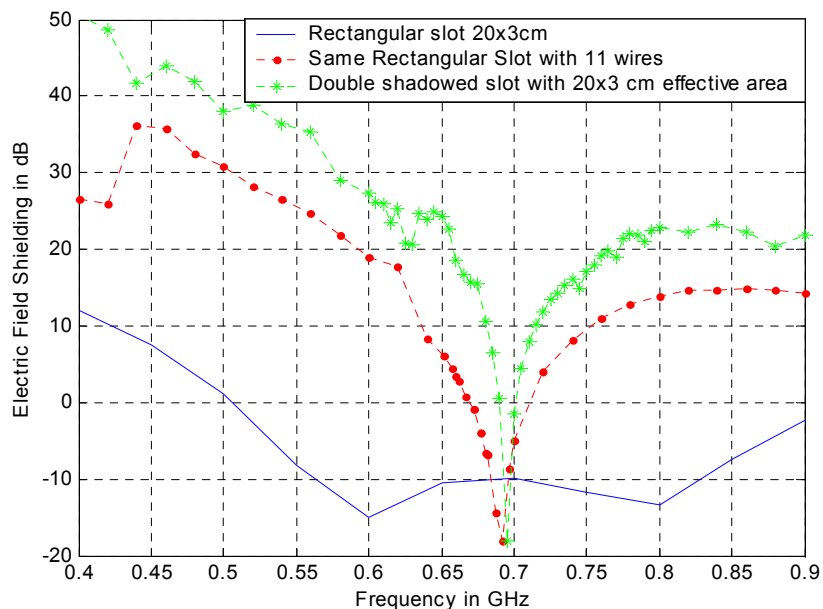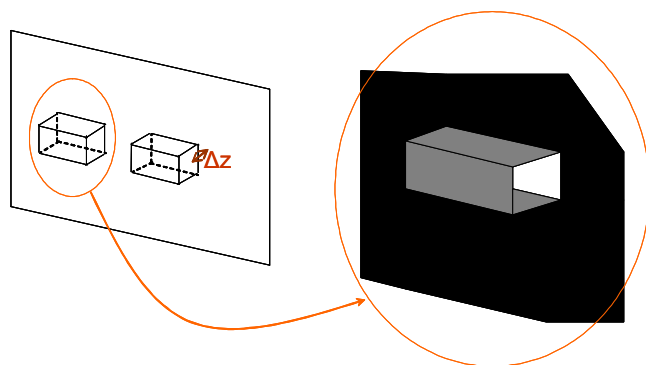
Comparison of slot shadowing with shielding wire array for ΔZ = 5cm
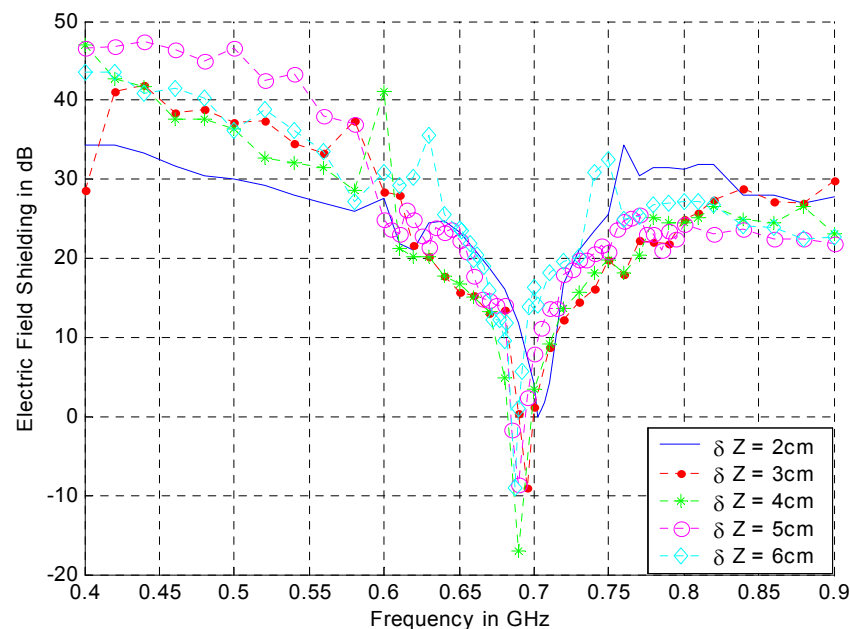
Variation in Distance ΔZ of PEC plate from Shadowed Slot

Effects of Cavity Loading

Electric Field Shielding

Legend:
- $R_c = 0$ (Metal)
- $R_c = 0.01 Z_0$
- $R_c = 0.05 Z_0$
- $R_c = Z_0 = 377\,\Omega$

Plot axes: EFS (dB) vs Frequency (GHz)

Diagram labels:
- 30 cm × 30 cm × 12 cm
- Resistive Cavity (R_c)
- Observation Point (Cavity Center)
- $\mathbf{E}^{inc}$, $\mathbf{k}$
- Rectangular Aperture (20 cm x 3 cm)
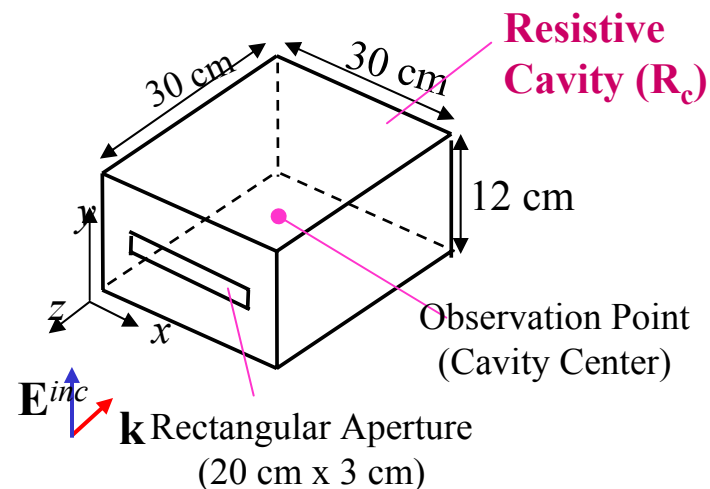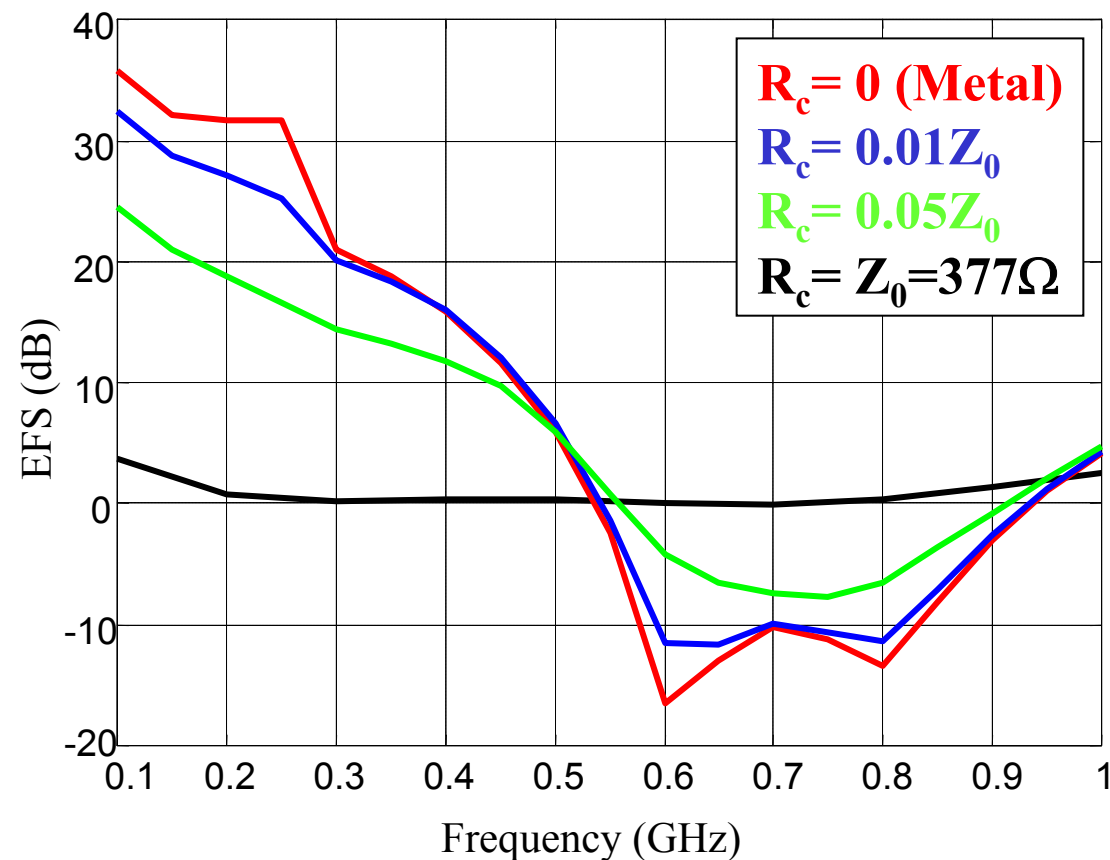
➢Low cost shielding using wire grids across the aperture can reduce coupling by 5 to 20 dB over the frequency range around the slot and cavity resonance.

➢ Using PEC plates to 'shadow' slots leads to a larger improvement of 5 to 30 dB over the same frequency range.

➢ Both approaches work on attenuating the incident wave and reducing the slot resonance so as to reduce EMC coupling.

➢ Cavity resonance at 0.7 GHz acts to amplify the input signal by as much as 10-20dB.

➢ Cavity resonance can be further attenuated by a sheet of dielectric within the cavity interior.

Excitation wave

Rectangular metallic cavity

Arbitrary shaped slot

$\overline{M1}$

Dielectric layer

Transmitted wave

$\overline{M2}$
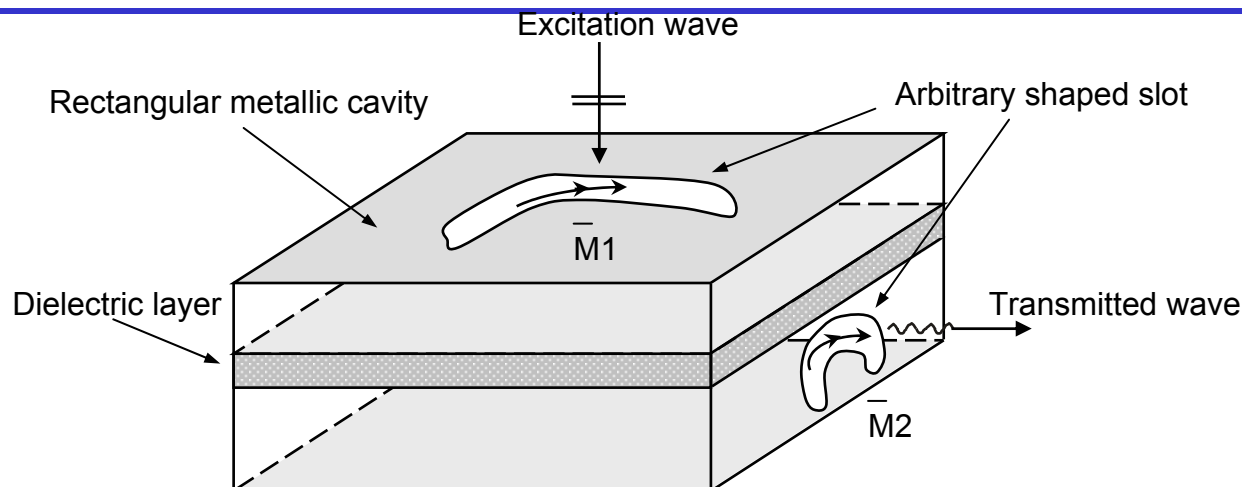
Why? To develop circuit models for incorporation into overall code

Excitation wave

Rectangular metallic cavity

Arbitrary shaped slot

$\overline{M}$

Microwave circuits

Dielectric layer

V_{-}^{+}

I

Port Analysis

Input port where $Y_{i,j}$ is measured

Excitation wave

Arbitrary shaped slot

Rectangular metallic cavity

$\overline{M}$

x

y

Dielectric layer

Admittance matrix account for interior (a) and exterior (b)
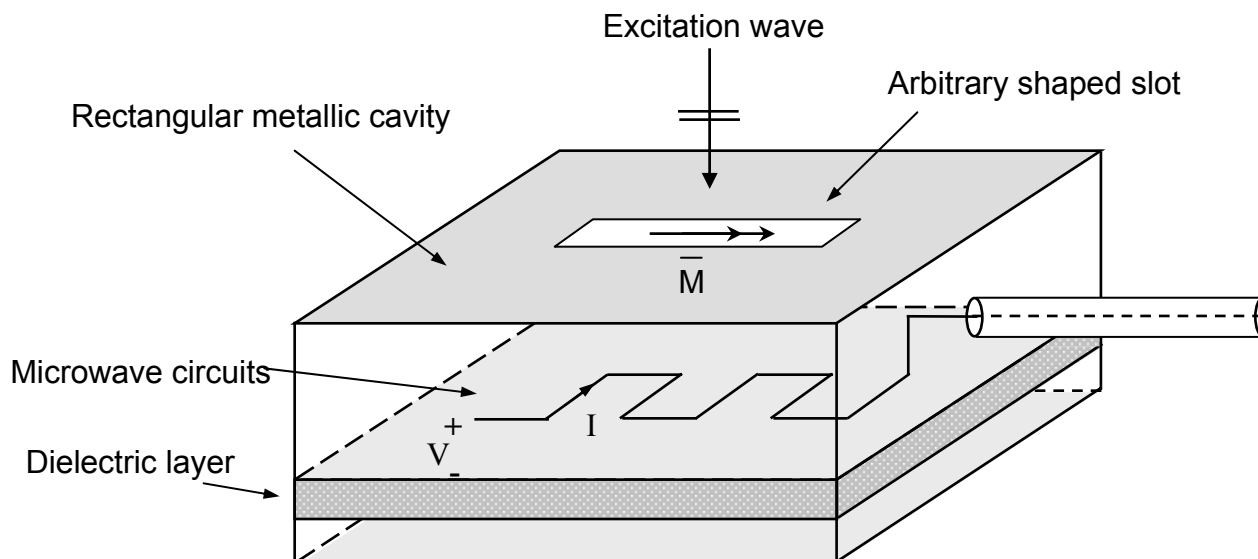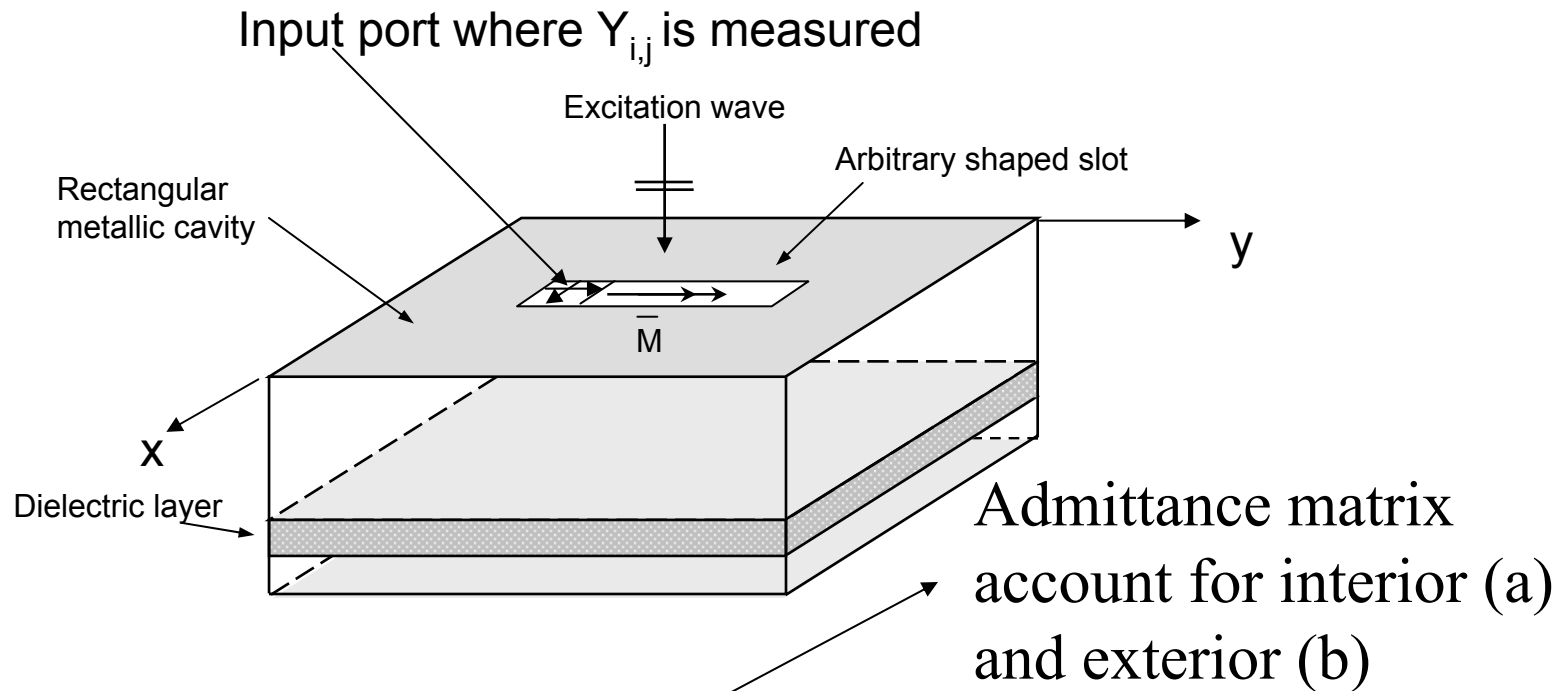
$$\begin{bmatrix} M_{xo} \\ M_{yo} \end{bmatrix} = -\begin{bmatrix} Y_{xx}^{a} - Y_{xx}^{b} & Y_{xy}^{a} - Y_{xy}^{b} \\ Y_{yx}^{a} - Y_{yx}^{b} & Y_{yy}^{a} - Y_{yy}^{b} \end{bmatrix}^{-1} \begin{bmatrix} I_{x}^{inc} \\ I_{y}^{inc} \end{bmatrix}$$

This column is very small

- Interior Fields

$$C_{mn} = -\frac{8jY_o(\Delta x \Delta y)^2}{k_o \mu_b \, ab} \frac{1}{k_{mn} \tan(k_{mn}c)}$$

$$H_x^b = \sum_{m,n} \frac{C_{mn}}{(2\Delta x \Delta y)^2} \left[\varepsilon_n \left\{ k_b^2 - \left(\frac{m\pi}{a}\right)^2 \right\} \int_S M_x \sin(\frac{m\pi}{a}x')\cos(\frac{n\pi}{b}y')ds' \right.$$

$$\left. - \varepsilon_m \left(\frac{m\pi}{a}\right)\left(\frac{n\pi}{b}\right) \int_S M_y \cos(\frac{m\pi}{a}x')\sin(\frac{n\pi}{b}y')ds' \right] \sin(\frac{m\pi}{a}x)\cos(\frac{n\pi}{b}y)$$

$$H_y^b = \sum_{m,n} \frac{C_{mn}}{(2\Delta x \Delta y)^2} \left[-\varepsilon_n \left(\frac{m\pi}{a}\right)\left(\frac{n\pi}{b}\right) \int_S M_x \sin(\frac{m\pi}{a}x')\cos(\frac{n\pi}{b}y')ds' \right.$$

$$\left. + \varepsilon_m \left\{ k_b^2 - \left(\frac{n\pi}{b}\right)^2 \right\} \int_S M_y \cos(\frac{m\pi}{a}x')\sin(\frac{n\pi}{b}y')ds' \right] \cos(\frac{m\pi}{a}x)\sin(\frac{n\pi}{b}y)$$

- Exterior Fields
                                                                          → Free space GF

$$\overline{H}^a(\overline{r}) = -jk_0Y_0 \int_S 2\overline{M}(r') \cdot \overline{\overline{\Gamma}}_0(\overline{r};\overline{r}')ds'$$

- Admittance matrix equation results by equating H fields at the aperture

Electric field shielding

Excitation wave

Rectangular metallic cavity

Arbitrary shaped slot

$\overline{M}$

Dielectric layer

Analytic

3 modes and 2 unknowns at aperture

loss: 10^{-10}
loss : 0.1
loss : 0.2
loss : 0.3
loss : 0.4

$-20\log(E^t/E^i)$

Freq. (GHz)

Excitation wave

Rectangular metallic cavity

Arbitrary shaped slot

$\overline{M1}$

Dielectric layer

Transmitted wave

$\overline{M2}$

30 cm

12 cm

30 cm

y

z

x

Ey

k

Rectangular Aperture 20 by 3 cm

Full Wave

MLFMM
Measured
FDTD

Electric Field Shielding in dB

Frequency in GHz

Antenna to Slot Coupling in Systems

Crossed Magnetic Dipole placed at the center of the antenna tray at car's back

Slot

Plane of points within car hood evaluated for EFS

Rectangular slot resonating at 0.7 GHz located at the dashboard
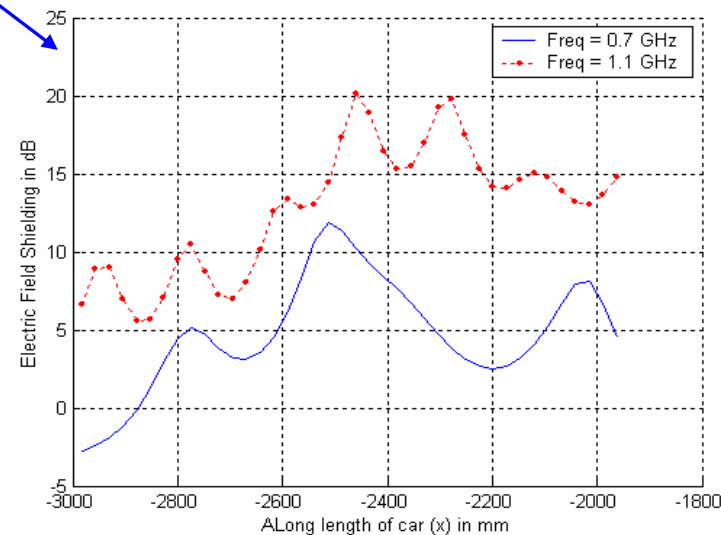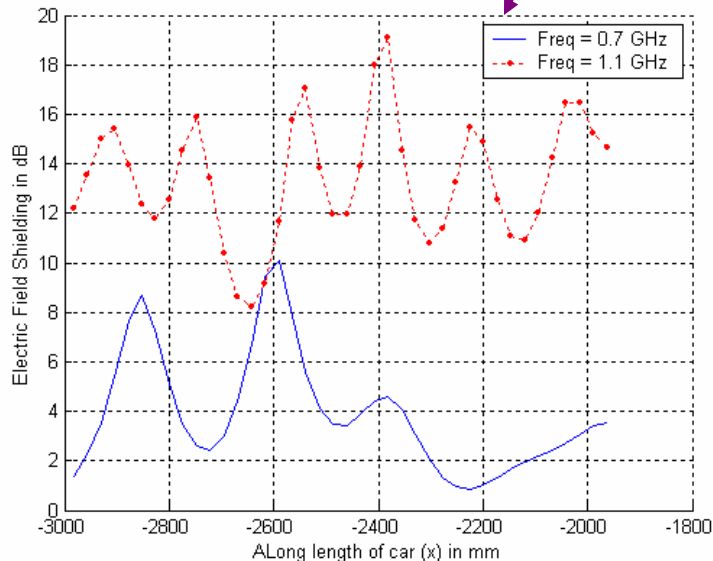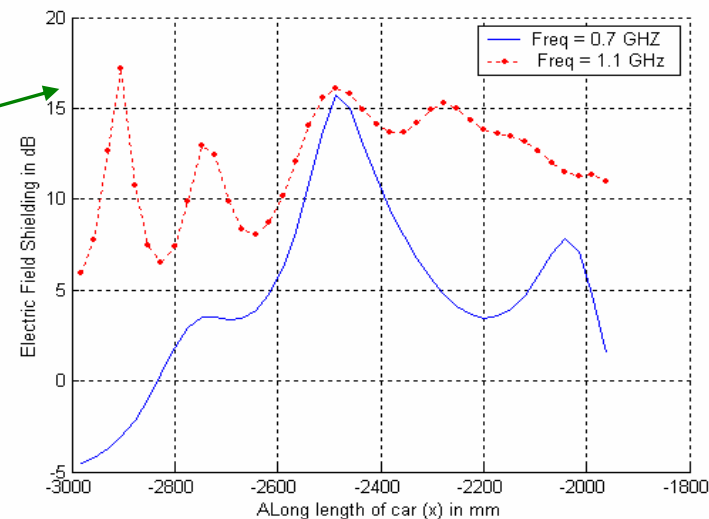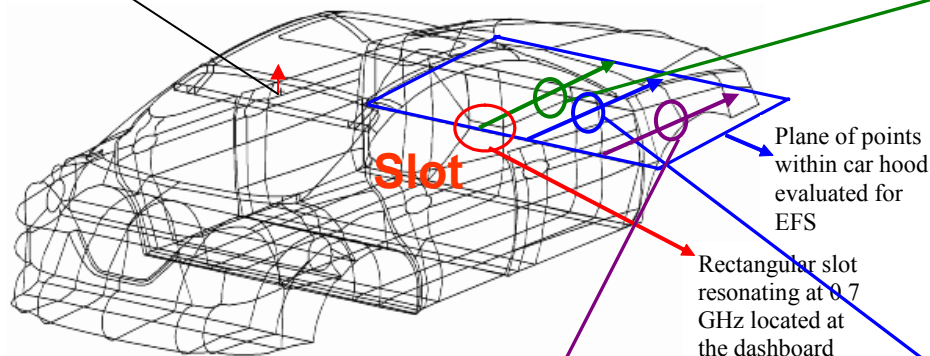
Front of Car

Dashboard

Slot is Resonating at 0.7 GHz

Overall Objective Function

$$F(x, y, z) = \frac{\sum\limits_{i=1}^{40} \left| E_i^{\,total} \right|^2}{\sum\limits_{i=1}^{40} \left| E_i^{\,inc} \right|^2}$$
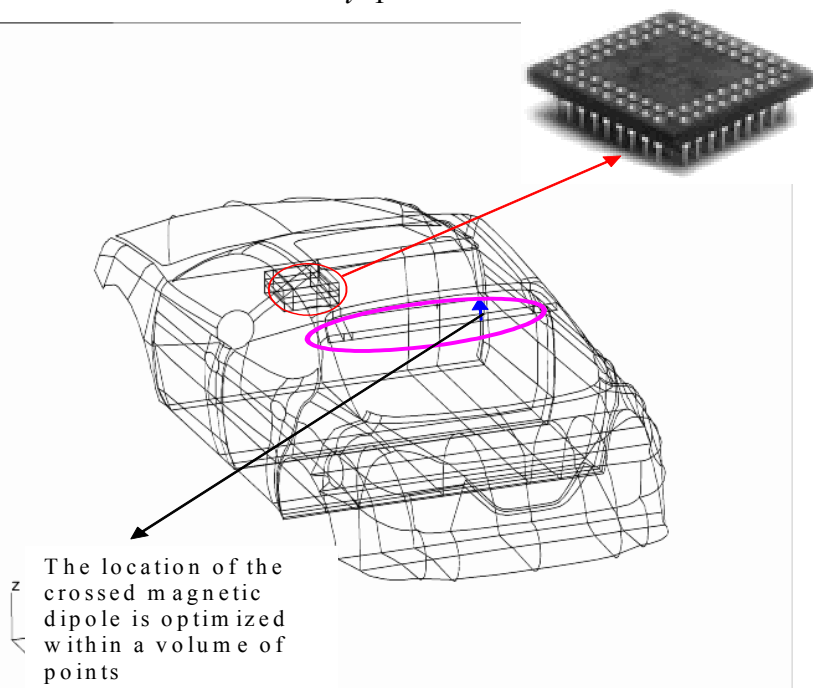

The location of the crossed magnetic dipole is optimized within a volume of points

➢ Excitation is a pair of crossed Magnetic dipoles with orthogonal phase excitation at 0.7 GHz (same as cavity).

➢ Antenna location is to be optimized for a volume of points on the back of an automobile that minimizes the EM Coupling from the antenna to the 40 pins of a chip placed within a resonant cavity.

➢ Resonant cavity at 0.7 GHz housing the electronic chip amplifies incident fields.

➢ Different antenna locations can mitigate cavity modal excitation and reduce EM coupling.

➢ Design space bounds: -70 ≤ x ≤ 70, -500 ≤ y ≤ 0 and -80≤ z ≤ 48.57

Left flowchart

Input variable values

↓

Analyzer Code such as MLFMM or FE-BI.

No – Check Mesh / Geometry file

Code Convergence?

Update new variable values

Yes ↓

Optimization Schemes such as SQP, GAs or SuperEGO with DIRECT on kriging surrogate modeling.
.

Termination tolerance met?

No

Yes -- Convergence

↓

Output Optimized variable values

Right flowchart
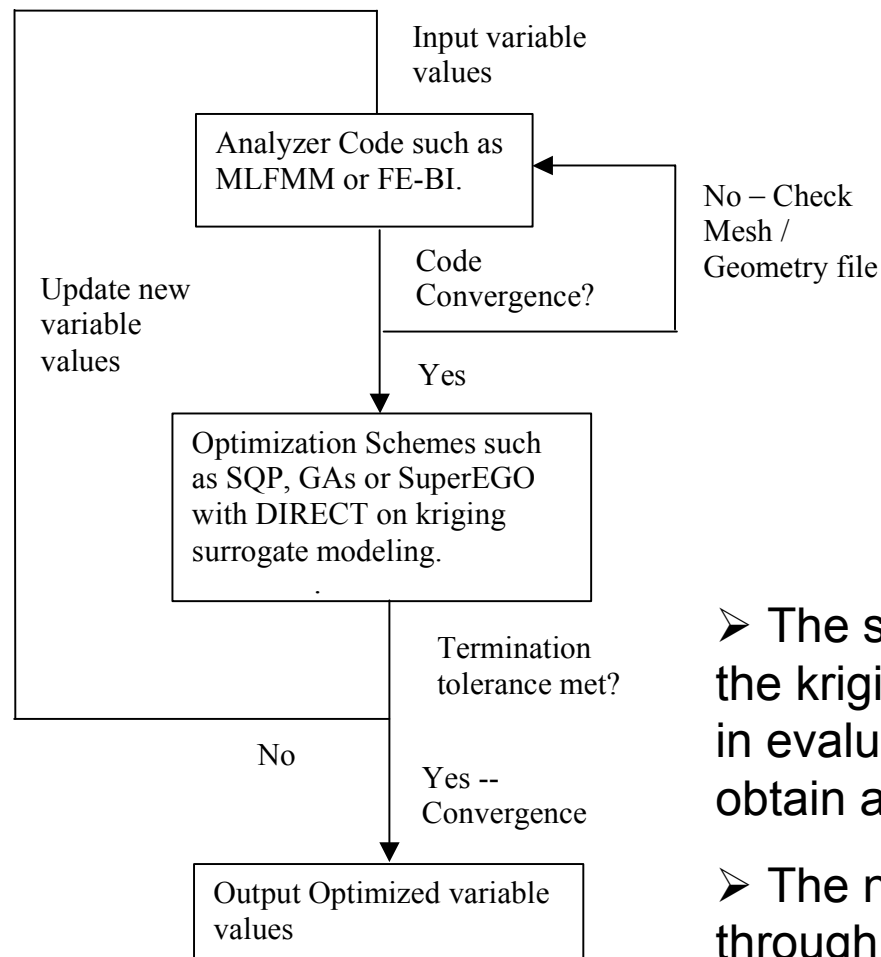
Flow Model of the superEGO Global Optimizer code

Take an initial Sample → Fit Kriging Models ↔ Choose appropriate kriging coefficients

Create Infill Sampling Criteria ↔ Optimize criteria using DIRECT

Up date Kriging Models

Predict next optimized iterate

Termination Criteria Met? — Yes → Stop

No
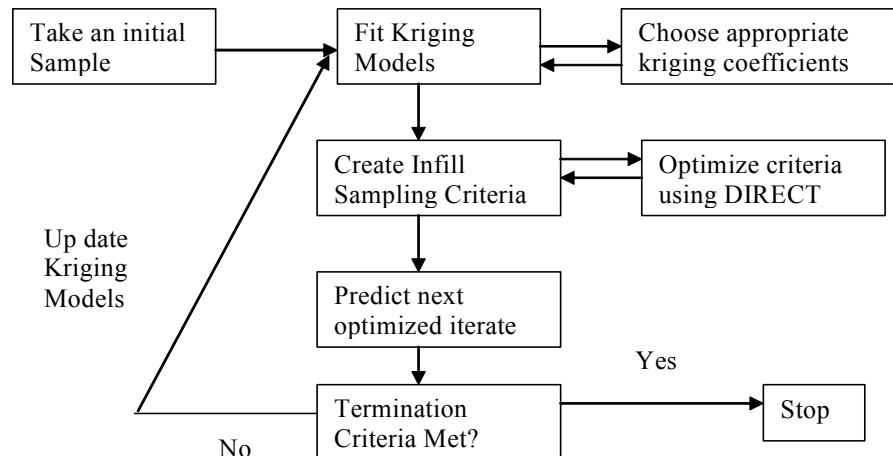
> The superEGO optimizer continually looks at the kriging meta-model to guide the optimizer in evaluating promising points with potential to obtain a low objective function.

> The next predicted design point is obtained through DIRECT to optimize an auxiliary model characterized by the choice of Infill sample criteria with kriging meta-modeling.

➢ Automobile model has 26000 unknowns, MLFMM code takes up 310 MBytes of RAM and solves in slightly over 2 hours on an SGI platform.

➢ Initial Kriging Model obtained from a sparse randomly generated vector of 18 data sampling points indicates a Response Surface with the presence of multiple local minima.
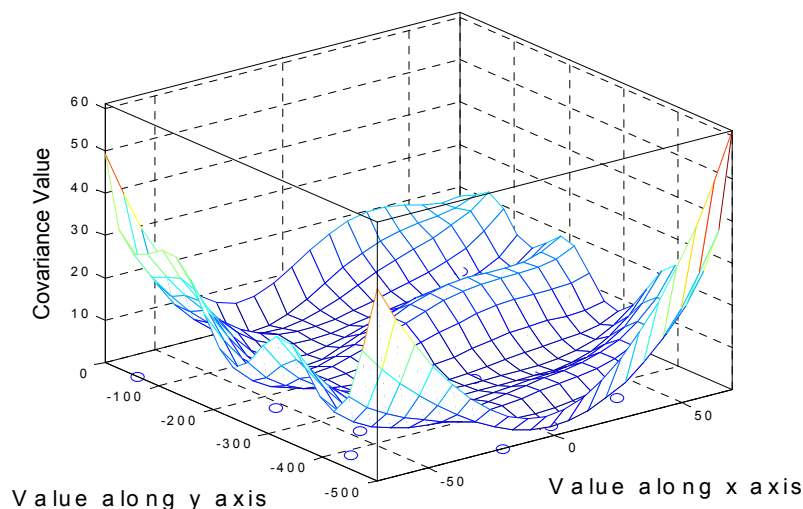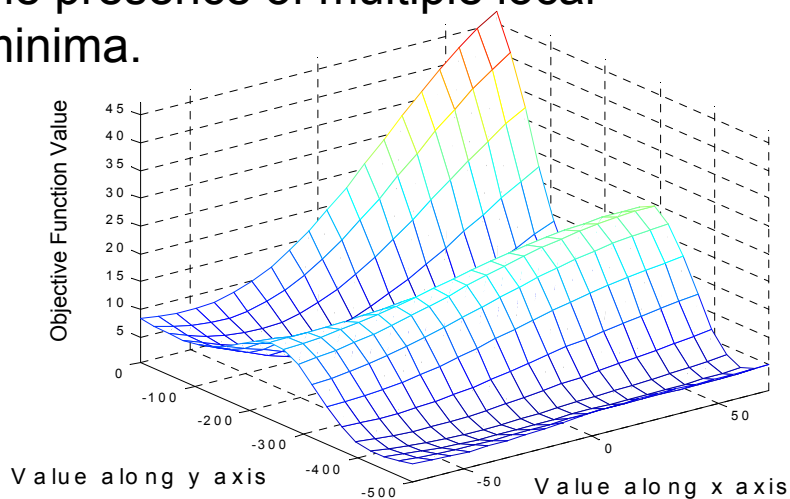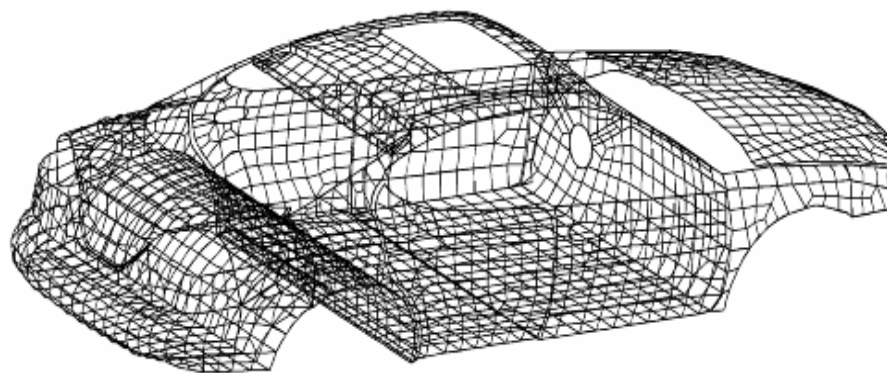
➢ Optimizer found a global minimum solution within tens of iterations besides the initial sample size. This is a significant improvement compared to using Genetic Algorithms.

➢ Using the Regional Extreme Infill Sampling criteria, local-global optimization scheme forces optimizer to find local minimum. Applying the Global optimization Infill scheme allows optimizer to find other global minimas.
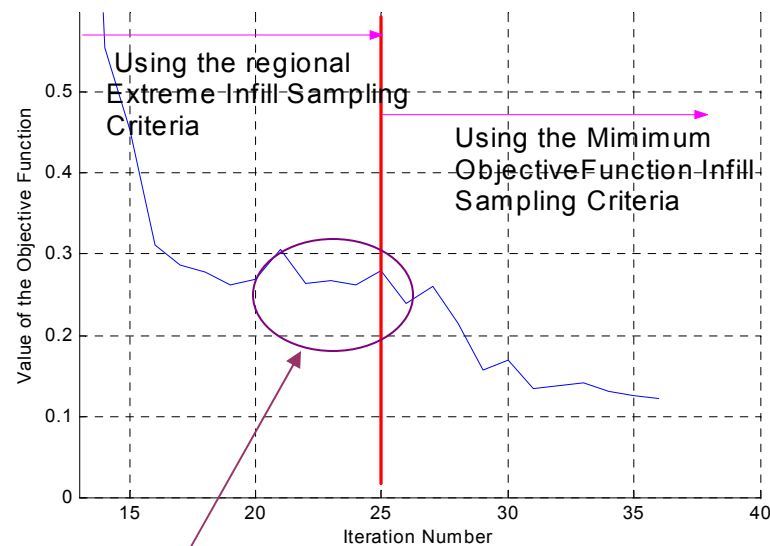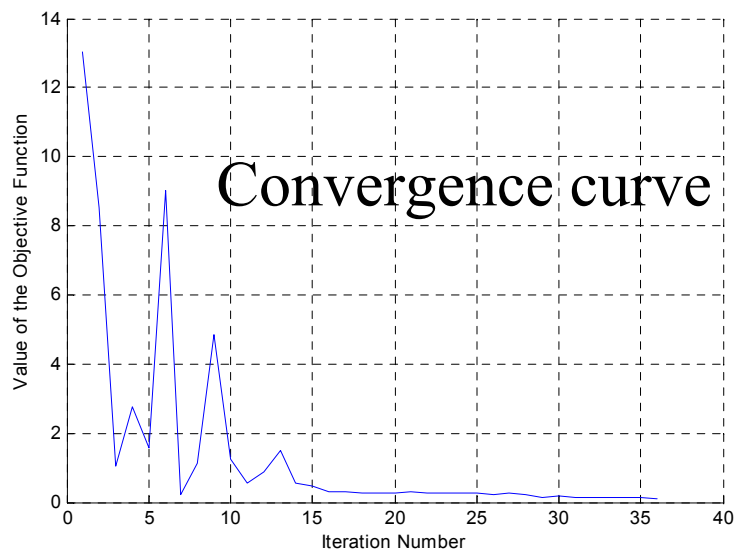

Region of local minimum Point

➢ Antenna location at the center of the automobile gives F(x,y,z) = 13.3025

➢ Final Optimized Antenna position gives F(x,y,z) = 0.122057 (20.37 dB improvement compared to the center location) at the positions x = 24.19753 mm, y = -421.773 mm and z = -34.6448 mm.

➢ Final kriging metamodel plots show a slightly modified Response Surface Modeling (RSM) with continual update of the kriging model at each optimization iteration.

Accomplishments
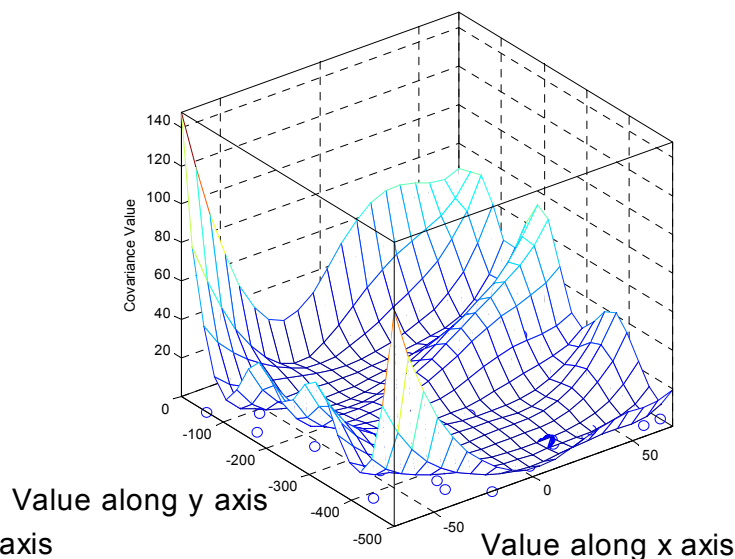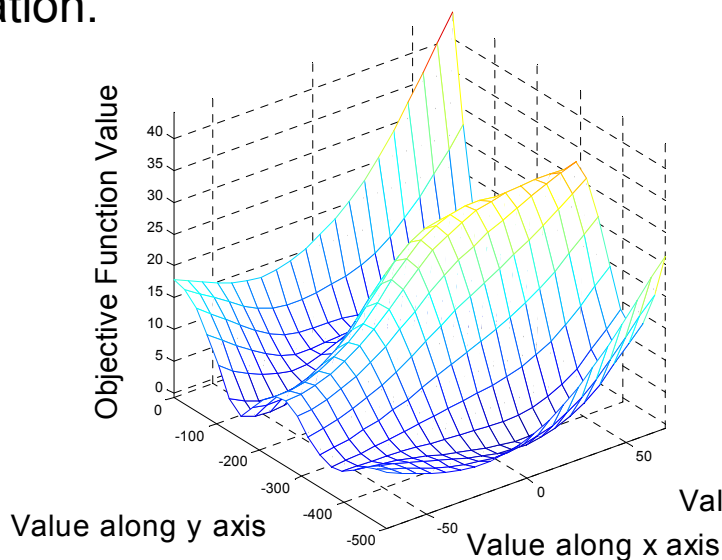
- Phenomenology of cavity coupling
- Effects of wire penetrations and loading
- Simplified semi-analytical model for cavity
- Coupling in systems using general-purpose EMCAR code
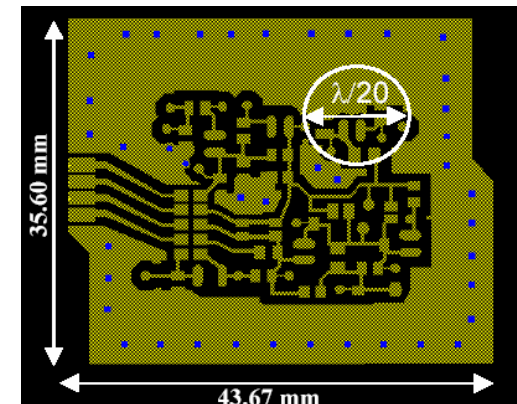- Optimization for coupling control in systems

Computational Tools

- MLFMM for coupling studies
- Hybrid (finite element, boundary/volume integrals) for modeling realistic systems

Next Steps
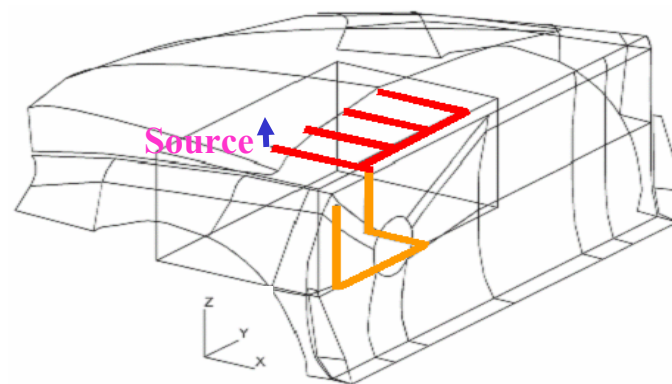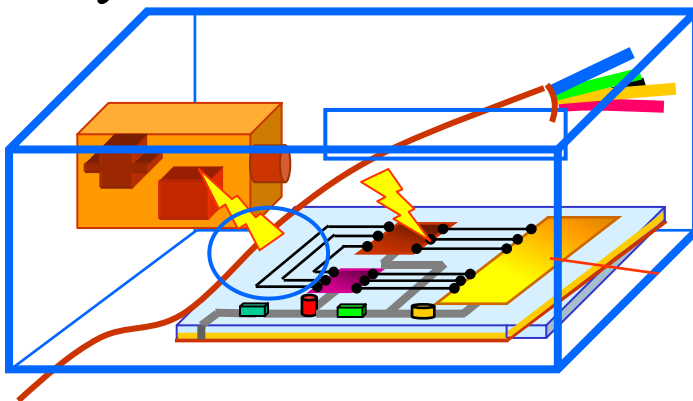
- Complete development of the hybrid FE-BI code with various Green's function domains.

- Further development of [Y] matrix model for integration

- **Modeling of realistic boards within enclosures**

Actual Interconnect

Interconnect Mesh

Grid Array Package

Digital Board